Published in final edited form as:
Neuroscience. 2007 April 25; 146(1): 286–297.

DISTRIBUTION OF SEROTONIN 5-HT$_{2C}$ RECEPTORS IN THE VENTRAL TEGMENTAL AREA

M. J. BUBAR and **K. A. CUNNINGHAM***
Center for Addiction Research, Department of Pharmacology and Toxicology, University of Texas Medical Branch, 301 University Boulevard, Galveston, TX 77555-1031, USA

Abstract

Serotonin 2C receptors (5-HT$_{2C}$R) appear to exert tonic inhibitory influence over dopamine (DA) neurotransmission in the ventral tegmental area (VTA), the origin of the mesolimbic DA system, thought to be important in psychiatric disorders including addiction and schizophrenia. Current literature suggests that the inhibitory influence of 5-HT$_{2C}$R on DA neurotransmission occurs via indirect activation of GABA inhibitory neurons, rather than via a direct action of 5-HT$_{2C}$R on DA neurons. The present experiments were performed to establish the distribution of 5-HT$_{2C}$R protein on DA and GABA neurons in the VTA of male rats via double-label immunofluorescence techniques. The 5-HT$_{2C}$R protein was found to be co-localized with the GABA synthetic enzyme glutamic acid decarboxylase (GAD), confirming the presence of the 5-HT$_{2C}$R on GABA neurons within the VTA. The 5-HT$_{2C}$R immunoreactivity was also present in cells that contained immunoreactivity for tyrosine hydroxylase (TH), the DA synthetic enzyme, validating the localization of 5-HT$_{2C}$R to DA neurons in the VTA. While the degree of 5-HT$_{2C}$R+ GAD co-localization was similar across the rostro-caudal levels of VTA subnuclei, 5-HT$_{2C}$R+TH co-localization was highest in the middle relative to rostral and caudal levels of the VTA, particularly in the paranigral, parabrachial, and interfascicular subnuclei. The present results suggest that the inhibitory influence of the 5-HT$_{2C}$R over DA neurotransmission in the VTA is a multifaceted and complex interplay of 5-HT$_{2C}$R control of the output of both GABA and DA neurons within this region.

Keywords

immunohistochemistry; GABA; dopamine; GAD-67; tyrosine hydroxylase

Evidence in the literature clearly indicates a role for the serotonin (5-HT) neurotransmitter system in modulating dopamine (DA) neurotransmission (Kapur and Remington, 1996). The serotonin 2C receptor (5-HT$_{2C}$R), a seventransmembrane G-protein-linked receptor that is widely expressed throughout the brain (Pompeiano et al., 1994), has emerged as one of the key players to mediate these 5-HT–DA interactions. Studies examining 5-HT$_{2C}$R modulation of DA neurotransmission have primarily focused upon interactions within the DA mesocorticoaccumbens pathways (for review, see Di Matteo et al., 2001), which originate in the ventral tegmental area (VTA) and terminate in the nucleus accumbens (NAc) and prefrontal cortex (PFC). These pathways are integral in mediating the rewarding and reinforcing properties of addictive drugs (Wise, 2005) as well as in the pathophysiology of psychosis (Winterer and Weinberger, 2004). Thus, the 5-HT$_{2C}$R may serve as important target for therapeutic intervention of these DA-mediated disease states (for review, see Bubar and Cunningham, 2006).

*Corresponding author. Tel: +1-409-772-9629; fax: +1-409-772-9642, E-mail address: kcunning@utmb.edu (K. A. Cunningham).

The 5-HT_{2C}R seems to exert a tonic and phasic inhibitory influence upon DA neurotransmission and DA-mediated behaviors (for review, see Bubar and Cunningham, 2006). For example, systemic administration of a 5-HT_{2C}R agonist decreases, while an antagonist increases, the firing rate of VTA DA neurons (Di Matteo et al., 1999). A primary site of action for the 5-HT_{2C}R to inhibit DA mesocorticoaccumbens neurotransmission may be via the 5-HT_{2C}R located within the VTA. Indeed, local administration of the 5-HT_{2C}R agonist RO 60–0175 into the VTA reduced stress-evoked DA release in the PFC (Pozzi et al., 2002), while intra-VTA administration of the 5-HT_{2C}R antagonist SB 242084 enhanced 3,4-methylenedioxymethamphetamine (MDMA)-evoked DA release in the NAc (Bankson and Yamamoto, 2004). Thus, the 5-HT_{2C}R within the VTA appears to provide an integral inhibitory influence upon DA neurotransmission, however, the mechanisms through which the 5-HT_{2C}R exerts this inhibition are unknown.

The VTA, located in the ventral portion of the mesencephalon, comprises the A10 population of mesencephalic DA neurons (Dahlstrom and Fuxe, 1964). A population of GABA neurons is also present within this region. These VTA GABA neurons appear to send collaterals that synapse locally on DA neurons within the VTA as well as projections that terminate in both the NAc (Van Bockstaele and Pickel, 1995) and/or PFC (Steffensen et al., 1998;Carr and Sesack, 2000). The mRNA (Pompeiano et al., 1994;Eberle-Wang et al., 1997) and protein (Abramowski et al., 1995;Clemett et al., 2000) for the 5-HT_{2C}R have been detected in the VTA and Eberle-Wang et al. (1997) reported that 5-HT_{2C}R mRNA in the VTA did not co-localize with mRNA for tyrosine hydroxylase (TH), the rate limiting enzyme for DA synthesis and a marker for DA neurons. This observation as well as the results of electrophysiological and microdialysis studies supports the hypothesis that the 5-HT_{2C}R is localized to GABA neurons, rather than DA neurons, within the VTA (Di Giovanni et al., 2000,2001;Di Matteo et al., 2001), however the distribution of 5-HT_{2C}R protein to GABA and DA neurons in the VTA has not been thoroughly investigated.

The goal of the present study was to examine the distribution of the 5-HT_{2C}R protein in the VTA via double-label fluorescence immunohistochemistry combining an anti-5-HT_{2C}R antibody (Bubar et al., 2005) with either an anti-glutamic acid decarboxylase (GAD) antibody to label GABA neurons, or an anti-TH antibody to label DA neurons in the VTA. Indeed, we not only report the first evidence to demonstrate the co-localization of 5-HT_{2C}R protein in VTA GABA neurons, but we also confirm the presence of 5-HT_{2C}R in a subpopulation of DA neurons in the VTA.

The VTA is a complex structure divided based upon cytoarchitecture into five subnuclei (see Fig. 1): the paranigral nucleus (PN), the parabrachial pigmented nucleus (PBP), the interfascicular nucleus (IF), the rostral linear raphe nucleus (RLi), and the caudal linear raphe nucleus (CLi). While, to our knowledge, there are no reports describing the characteristics of GABA cell populations within the different subnuclei, the cell morphology of the DA neurons as well as their afferent and efferent projections have been shown to differ across the subnuclei (Phillipson, 1979;Swanson, 1982). Thus, subsequent to the initial detection of 5-HT_{2C}R co-localization with both GABA and DA neuronal markers, we conducted a detailed analysis of 5-HT_{2C}R distribution and co-localization with TH and GAD in subnuclei throughout the rostro-caudal extent of the VTA.

EXPERIMENTAL PROCEDURES

Tissue preparation

Naïve male Sprague–Dawley rats (*N*=6; 175–199 g; Harlan Sprague–Dawley, Inc., Houston, TX, USA) were used. Rats were deeply anesthetized with pentobarbital (100 mg/kg, i.p., Sigma-Aldrich, St. Louis, MO, USA) and perfused transcardially with phosphate-buffered

saline (PBS) followed by 3% paraformaldehyde in PBS. Brains were removed, blocked at mid-pons, and post-fixed for 2 h at room temperature (RT). Brains were then cryoprotected in 30% sucrose for 48 h at 4 ºC, rapidly frozen on crushed dry ice, and stored at −80 ºC until sectioning. All experiments conformed to the *NIH Guide for the Care and Use of Laboratory Animals* (National Institutes of Health, 1986) and were approved by the UTMB Institutional Animal Care and Use Committee. All efforts were made to minimize the number of animals used and their suffering.

Coronal sections (20 μm) containing the VTA (−4.8 through −6.5 from Bregma) were taken from each brain using a cryostat (Leica CM 1850 at 20 ºC; Leica Microsystems, Bannockburn, IL, USA) according to the atlas of Paxinos and Watson (1998). Free floating sections were processed as described below.

Antibodies

Based on our previous validation of its selectivity for the 5-HT_{2C}R (Bubar et al., 2005), the commercially available goat polyclonal anti-5-HT_{2C}R antibody (1:100; sc-15081, Santa Cruz Biotechnology, Santa Cruz, CA, USA) was utilized for the present experiments. To assess co-localization of the 5-HT_{2C}R in DA or GABA neurons, the anti-5-HT_{2C}R antibody was used in combination with a mouse monoclonal anti-TH antibody (1:3000; #22941, Immunostar, Hudson, WI, USA) or a rabbit polyclonal anti-GAD 67 (1:150; sc-5602; Santa Cruz), respectively. The fluorescent secondary antibodies (1:2000; Molecular Probes, Eugene, OR, USA) used to visualize the proteins included the Alexa Fluor 488 donkey anti-goat (A-11055), Alexa Fluor 555 donkey anti-mouse (A-31570), and Alexa Fluor 555 donkey anti-rabbit (A-31572).

Immunofluorescence

Free floating brain sections were washed using an orbital shaker in PBS (2×10 min), then incubated in 20 mM sodium acetate (15 min), and washed again (3×10 min) with PBS. The sections were then incubated in a blocking serum [1.5% normal donkey serum (ImmunoResearch Laboratories, Inc., West Grove, PA, USA)] for 1 h at RT. The blocking serum was aspirated, and the sections were then incubated on an orbital shaker with primary antibodies diluted in 1.5% normal donkey or goat serum for 44 h at 4 ºC. The sections were then washed with PBS and incubated with the secondary antibodies diluted in 1.5% normal donkey or goat serum for 1 h RT, protected from light. Sections were washed with PBS (3×10 min) and mounted using a 0.1% Dreft® solution onto gelatin chrom alum-coated slides. The slides were then coverslipped using Vectashield® fluorescent mounting medium with DAPI (4′,6-diamidoino-2-phenylindole; Vector Laboratories, Burlingame, CA, USA), and stored protected from light at 4 ºC until viewing.

For each combination of primary and secondary antibodies, no primary or secondary antibody, no primary antibody, and mis-matched primary/secondary antibody (e.g. goat anti-5-HT_{2C}R +donkey anti-mouse secondary, etc.) control experiments were conducted to examine, respectively, tissue autofluorescence, non-specific secondary antibody binding, and cross-reactivity between primary and secondary antibodies raised in/against different species. Experiments conducted in the absence of primary and/or secondary antibody revealed the presence of some auto-fluorescence and non-specific secondary antibody labeling (data not shown); this staining, however, was minimal compared with the intense immunoreactivity (IR) detected following the appropriate anti-5-HT_{2C}R, anti-GAD or anti-TH antibody/secondary antibody combinations. Simultaneous application of the anti-5-HT_{2C}R and anti-GAD or anti-TH antibodies in double-label experiments did not alter the pattern of staining of either antibody as observed by comparison to IR staining in single-label experiments (data not shown). Control experiments using mis-matched primary and secondary antibody combinations (e.g. goat

anti-5-HT_{2C}R antibody+donkey anti-rabbit secondary antibody) resulted in IR levels similar to background IR detected in control (no-primary and/or secondary antibody) experiments revealing no cross-reactivity between antibodies of different species (data not shown).

Image analysis

Digital images were captured from brain sections using an Olympus BX51 fluorescent microscope (Olympus, Melville, NY, USA) equipped with a Hamamatsu camera (C4742-95; Hamamatsu, Bridgewater, NJ, USA) interfaced to a personal computer and were analyzed using Simple PCI software (version 5.1, Compix Inc., Imaging Systems, Cranberry Township, PA, USA). A 20× or 40× objective was used to capture all photomicrographs for final magnification of 400 and 800, respectively. Green fluorescence emitted by the Alexa Fluor 488 antibody was visualized using a yellow GFP filter set (# 41017; Chroma Technology Corporation, Rockingham, VT, USA), while the red fluorescence emitted by the Alexa Fluor 555 antibodies was visualized using a narrow band green excitation filter set (U-MNG2, Olympus). In addition, DAPI staining was visualized using a Blue GFP II filter set (#31041, Chroma).

For each tissue section, three images of the same viewing area were captured, one for each filter set detecting IR for each antibody and DAPI, and then resultant images were overlaid. Antibody-specific IR was defined as IR that was visible in tissue sections labeled with the appropriate primary–secondary antibody concentration, but was not detectable in the presence of either the primary or secondary antibody alone. The contrast of each image was adjusted to eliminate background staining; contrast settings differed for each antibody combination utilized and were based upon the level of background staining in the control sections that were processed simultaneously for each brain analyzed.

Rostro-caudal patterns of 5-HT_{2C}R-IR staining colocalized with TH-IR and GAD-IR staining in the VTA were analyzed for the five subnuclei of the VTA: PN, PBP, IF, RLi, and CLi (Swanson, 1982), according to Bregma locations described in Fig. 1 and Table 1 (Paxinos and Watson, 1998). Two to five 5-HT_{2C}R+TH-labeled sections and adjacent (when possible) 5-HT_{2C}R+GAD-labeled sections per rostro-caudal level were examined from each rat (n=3) for a range of 7 to 12 total sections per level for analysis of TH- and GAD-IR and 15–22 sections per level for analysis of 5-HT_{2C}R-IR. For each section, a composite photomicrograph composed of 20–30 individual images captured using the 20× objective was assembled to visualize the entire VTA. In an effort to minimize the differences in the sizes and shapes of the subnuclei throughout the rostro-caudal levels, rectangular areas of a fixed size were utilized to count cells within each subnucleus for all sections at the same magnification.

The location of each subnucleus was readily identified based on the morphology and orientation of the TH-IR or GAD-IR cells (Phillipson, 1979;Swanson, 1982;Domesick et al., 1983) and in reference to the location of the mammary peduncles (MP) and the fasciculus retroflexus (fr) in rostral sections and the interpeduncular nucleus (IP) in middle and caudal sections (Paxinos and Watson, 1998). Rectangular areas were positioned within each identified subnuclear region of interest, while avoiding transition areas between subnuclei and surrounding brain regions such as the substantia nigra. Two separate regions of similar size (64.52 cm^2 each) were used in all levels for the PN and PBP, while a single region was used for the IF (58.06 cm^2), RLi (58.06 cm^2), and CLi (64.52 cm^2). Cells contained in each rectangular area were counted using the “Region of Interest” function of the Simple PCI software, which enabled selection of IR cells according to the intensity and area of each signal. First, the number of singlelabeled cells was counted for each different color label (red and green), then the same parameters used for each single label were applied to the overlay image to determine the number of double-labeled cells.

The total number of 5-HT_{2C}R-IR, TH-IR, and GAD-IR cells was averaged (mean±S.E.M.) for rostral, middle, and caudal levels of each subnucleus; however, because of the geometric variations between the subnuclei and the areas measured, comparisons of the total cells detected could not be made between subnuclei; rather, comparisons were only made between the different rostro-caudal levels of a given subnucleus. Additionally, for each section, the percentage of 5-HT_{2C}R+TH-IR or 5-HT_{2C}R+GAD-IR co-labeled cells was determined by averaging the number of 5-HT_{2C}R+TH-IR or 5-HT_{2C}R+GAD-IR-co-labeled cells divided by the total number of TH-IR or GAD-IR cells, respectively. The resultant values were averaged (mean±S.E.M.) for rostral, middle, and caudal levels of each subnucleus. Individual one-way analysis of variance (ANOVA) was utilized to examine differences in the percentages of total TH- or GAD-IR cells co-labeled with 5-HT_{2C}R-IR within: 1. the different subnuclei in each rostro-caudal level, and 2. the different levels of each subnucleus (Fite et al., 2005). Significant main effects were followed with post hoc analysis using the Student-Newman-Keuls procedure (Keppel, 1973). Unpaired two-tailed *t*-tests were utilized to examine the rostro-caudal differences in IF, RLi, and CLi, since these subnuclei are only represented at two rostro-caudal levels. All statistical analyses were performed using GraphPad InStat (version 3.01; GraphPad Software, San Diego CA, USA); $P<0.05$ was the criterion to determine statistical significance.

To verify the observation of co-localization of 5-HT_{2C}R+TH, double-labeled sections were also viewed in the UTMB Infectious Disease and Toxicology Optical Imaging Core using a Zeiss LSM 510 META UV laser scanning confocal microscope equipped with a C-aphochromat 63×/1.2 water immersion objective (Carl Zeiss Microimaging, Thornwood, NY, USA). Sets of images were captured with the LSM5 Imaging Software (Carl Zeiss Microimaging) using two different fluorescent filter sets to detect the individual fluorophores and the resultant images were overlaid. A series of 10 consecutive image sets were captured at approximately 2 μm intervals through the depth of the 20 μm section of the VTA.

RESULTS

5-HT_{2C}R-IR in the VTA

Intense 5-HT_{2C}R-IR was observed throughout the rostral (Fig. 1B), middle (Fig. 1E), and caudal levels (Fig. 1H) of all subnuclei in the VTA. The 5-HT_{2C}R-IR in each subnucleus was most prominently expressed in cell bodies (Fig. 1C, F, I, arrows), although labeling of neuronal processes was also detected (Fig. 1C, F, I, arrowheads) particularly within the PBP, RLi, and CLi, albeit less frequently. Furthermore, tiny clusters of 5-HT_{2C}R-IR much smaller in diameter than the cell bodies were also observed (see open arrows, Figs. 2E and 3E, middle column). These small clusters, which may be indicative of terminal boutons, were most commonly present within the IF, RLi and CLi. Although all three patterns of staining were present throughout the VTA, analysis was focused upon the detection of 5-HT_{2C}R-IR in cell bodies, as this type of staining could be consistently and reliably detected and quantified.

As described in Table 1, the relative number of 5-HT_{2C}R-IR cells detected in the rostro-caudal levels of each region of interest for a given subnucleus was as follows: PBP and PN (middle>rostral>caudal), IF (middle>caudal) and RLi (rostral=middle); the CLi is only present in the caudal level.

GAD- and TH-IR in the VTA

Both GAD- (Fig. 2A; B–E, left column) and TH-IR cells (Fig. 3A; B–E, left column) and processes were clearly visible in each of the subnuclei throughout the rostro-caudal extent of the VTA. The morphology and patterns of orientation of GAD- and TH-immunopositive cells were similar, and subnuclei were readily distinguished with either type of staining (Figs. 2A, 3A). Briefly, GAD- (Fig. 2B, left) and TH-IR cells (Fig. 3B, left) in the IF were spherical and

tightly packed. Both GAD- (Fig. 2C, left) and TH-IR cells (Fig. 3C, left) in the PN subnucleus were large and typically oriented horizontally, following along the IP located ventral to the VTA in middle and caudal sections. The GAD- (Fig. 2D, left) and TH-IR cells (Fig. 3D, left) in the PBP, while also large, were spread diffusely with no particular orientation. In the RLi, located just dorsal to the IF, GAD- and TH-IR cells were less densely packed, but similar in size or slightly larger than labeled cells in the IF, and displayed a dorsal–ventral orientation (Figs. 2E and 3E, left). Cells in the CLi (present only in the caudal VTA) were similar in size and orientation to the GAD- and TH-IR cells in the RLi (data not shown). These morphological and orientation characteristics are analogous to those described previously for TH- and non-TH IR cells in the VTA (Phillipson, 1979;Swanson, 1982;Domesick et al., 1983;Nocjar et al., 2002).

Although GAD- vs. TH-IR cells could not be distinguished based on morphological characteristics, the distribution of IR staining throughout the subnuclei and rostro-caudal levels of the VTA differed slightly between the two cell types. GAD-IR cells were equally distributed throughout the different rostro-caudal levels of each region of interest for a given subnucleus, except for in the IF, where more cells were detected in the middle vs. rostral level, and in the PN where fewer cells were detected in the caudal vs. rostral or middle levels (Table 1). TH-IR cells, on the other hand, were differentially distributed among the rostro-caudal levels of each region of interest for a given subnucleus as follows: PBP (rostral=middle>caudal) PN (middle>rostral>caudal), IF (middle>rostral), RLi (rostral=middle) (Table 1). When comparing the density of TH- vs. GAD-IR cells in each region of interest for a given subnucleus (Table 1), TH-IR cells were more prominent than GAD-IR cells in all levels of the IF, PBP, and CLi, and the middle PN, while approximately equal numbers of GAD-and TH-IR cells were observed in both levels of the Rli and in the rostral and caudal PN.

Co-labeling for the 5-HT_{2C}R+GAD

In all VTA subnuclei examined there were cells that contained only 5-HT_{2C}R-IR (Fig. 2; green), cells that contained only GAD-IR (Fig. 2; red) as well as those that contained both 5-HT_{2C}R+GAD-IR (Fig. 2, right column; yellow; closed arrows). Thus, the 5-HT_{2C}R-IR was co-localized in a subset of GAD-IR cells. In addition, as noted above, punctate clusters of 5-HT_{2C}R-IR were frequently observed; these 5-HT_{2C}R-IR clusters tended to either form "strings" of IR that tracked along GAD-IR processes (Fig. 2; arrowheads) or the 5-HT_{2C}R-IR clusters were found to co-label with punctate clusters of GAD-IR (Fig. 2; open arrows), which may reflect the presence of co-labeled terminal boutons.

The extent of co-localization of 5-HT_{2C}R+GAD-IR varied slightly among the VTA subnuclei, ranging from ~21–37% of total GAD-IR cells detected within the regions of interest (Fig. 4A). When comparing the percentage of 5-HT_{2C}R+GAD-IR cells across the regions of interest for the various subnuclei at each rostro-caudal level, there was not a main effect of subnucleus location on the percentage of 5-HT_{2C}R+GAD-IR cells within the rostral ($F_{3,38}$=1.84; P=0.16), middle ($F_{3,36}$=1.84; P=0.77), or caudal levels ($F_{2,20}$=0.26; P=0.77; Fig. 4A), suggesting that similar percentages of co-labeling were detected among all subnuclei at a given rostro-caudal level. However, when the proportion of 5-HT_{2C}R+GAD-IR cells was compared across rostro-caudal levels of each region of interest for a given subnucleus, there was a main effect of rostro-caudal level on the percentage of 5-HT_{2C}R+GAD-IR cells in the PBP ($F_{2,24}$=3.55; P<0.05), reflecting higher proportions of 5-HT_{2C}R+GAD-IR cells in the middle PBP compared with rostral PBP (see # in Fig. 4A).

Co-labeling for 5-HT_{2C}R+TH

In all VTA subnuclei examined, cells that contained only 5-HT_{2C}R-IR (Fig. 3; green), only TH-IR (Fig. 3; red) as well as those that contained both 5-HT_{2C}R-IR+TH-IR (Fig. 3, right

column; yellow; closed arrows) were observed. Thus, the 5-HT_{2C}R-IR was co-localized in a subset of TH-IR cells. In addition, as noted above, punctate clusters of 5-HT_{2C}R-IR were frequently observed; these 5-HT_{2C}R-IR clusters tended to either form "strings" of IR that tracked along TH-IR processes (Fig. 3; arrowheads) or the 5-HT_{2C}R-IR clusters were found to co-label with punctate clusters of TH-IR (Fig. 3; open arrows), which may reflect the presence of co-labeled terminal boutons. The presence of 5-HT_{2C}R-IR within TH-IR cells was confirmed through examination of the images captured on a confocal microscope (Fig. 5), which demonstrated the presence 5-HT_{2C}R-IR throughout the cell membrane and cytoplasm of TH-IR (Fig. 5, arrows) and non-TH-IR cell bodies (Fig. 5, arrowheads).

The extent of co-localization for 5-HT_{2C}R+TH-IR within the various VTA subnuclei ranged from ~17–48% of total TH-IR cells detected (Fig. 4B). Comparisons of the percentage of 5-HT_{2C}R+TH-IR cells across the various subnuclei at each rostro-caudal level revealed a main effect of subnucleus location on the percentage of 5-HT_{2C}R+TH-IR cells in the middle ($F_{3,39}$=5.52; P<0.01) and caudal levels ($F_{2,20}$=4.34; P<0.01), but not the rostral level of the VTA ($F_{3,40}$=2.06; P=0.12; Fig. 4B). In the middle VTA, a significantly higher proportion of total TH-IR cells were co-labeled for 5-HT_{2C}R-IR in the IF, PN and PBP subnuclei relative to the RLi subnucleus (see * in Fig. 4B). In the caudal VTA, a significantly higher percentage of 5-HT_{2C}R+TH-IR cells was detected in the CLi compared with the PN (see @ in Fig. 4B).

When comparing the proportion of 5-HT_{2C}R+TH-IR cells across the rostro-caudal levels of each subnucleus, a main effect of rostro-caudal level on the percentage of co-labeled cells in each subnucleus was observed for the IF (t_{20}=4.10; P<0.001), PN ($F_{2,27}$=14.47; P=0.001) and PBP ($F_{2,27}$=7.49; P<0.01; Fig. 4B). A significantly higher proportion of 5-HT_{2C}R+TH-IR cells was observed in the middle IF compared with rostral IF (see # in Fig. 4B) as well as the middle PN compared with rostral PN (see # in Fig. 4B). Additionally, a significantly lower percentage of 5-HT_{2C}R+TH-IR cells was observed in the caudal PN and PBP compared with the rostral (see # in Fig. 4B) or middle (see in Fig. 4B) PN and PBP, respectively.

DISCUSSION

The present study is the first to quantify the occurrence of 5-HT_{2C}R-IR co-localized to subsets of GAD- *and* TH-IR cells throughout the VTA subnuclei. The data reveal that the 5-HT_{2C}R is located on subpopulations of *both* GABA and DA neurons in the VTA. While the percentage of 5-HT_{2C}R co-localization with GAD-IR was relatively similar across the levels of the various subnuclei, the proportion of TH-IR cells co-labeled with 5-HT_{2C}R-IR differed significantly across a number of subnuclei, with the greatest incidence of co-localization occurring in the middle levels of the VTA. These findings indicate that the 5-HT_{2C}R regulation of VTA neuronal function is more complex than previously thought, potentially involving both direct and indirect modulation of the output of DA mesocorticoaccumbens circuits by the 5-HT_{2C}R.

5-HT_{2C}R distribution

Several studies have reported low to moderate levels of 5-HT_{2C}R mRNA in the VTA (Hoffman and Mezey, 1989;Mengod et al., 1990;Pompeiano et al., 1994;Wright et al., 1995;Eberle-Wang et al., 1997). The highest 5-HT_{2C}R mRNA expression was observed in mid to caudal levels of the VTA, particularly in the CLi (Eberle-Wang et al., 1997). A similar gradient of 5-HT_{2C}R mRNA expression has also been reported in the substantia nigra, where 5-HT_{2C}R mRNA expression is higher in caudal vs. rostral levels of the substantia nigra (Eberle-Wang et al., 1997). Likewise, the present study revealed a gradient of 5-HT_{2C}R protein expression in the VTA, although the highest levels of 5-HT_{2C}R-IR were observed in the middle levels of the VTA, with lower 5-HT_{2C}R expression in more caudal levels.

Consistent with previous studies reporting high levels of 5-HT_{2C}R protein in the ventral mesencephalon of rats (Mengod et al., 1990;Clemett et al., 2000; but see Li et al., 2004), the present study revealed that the 5-HT_{2C}R protein is widely expressed in all subnuclei throughout the rostro-caudal extent of the VTA, perhaps to a greater extent than would be predicted based on levels of 5-HT_{2C}R mRNA expression in this region (Eberle-Wang et al., 1997). A number of variables stochastically drive gene induction to give rise to multiple patterns of protein expression than predicted by a simple one-for-one relationship for mRNA to protein molecule (Cai et al., 2006;Zhang et al., 2006). Thus, the 5-HT_{2C}R protein expression may reflect the activity of a small number of mRNA molecules, with expression levels determined by variables such as translational efficacy, lifetime of active promoter and mRNA and protein turnover rates. Furthermore, experimental variables, such as differences in the detection sensitivity among *in situ* hybridization vs. immunohistochemical assays may also contribute to the disparate 5-HT_{2C}R mRNA and protein expression observed in the VTA. Mismatched expression of 5-HT_{2C}R mRNA and protein has been reported for other brain areas, including the caudate-puta-men and the central gray (Mengod et al., 1990;Clemett et al., 2000). In these brain areas, the pattern of low mRNA and high protein expression was proposed to indicate high levels of pre-synaptic (terminal) location of the receptors (Mengod et al., 1990;Clemett et al., 2000). In the present study, some of the 5-HT_{2C}R-IR observed was indicative of terminal bouton labeling (see open arrows, Figs. 2E and 3E, middle column); however, the presence of 5-HT_{2C}R-IR throughout the cell soma (including cytoplasm) as observed in confocal images (see Fig. 5), indicates primarily post-synaptic localization of the receptor. Thus, while presynaptic localization of the 5-HT_{2C}R may account in part for disparate distributions of mRNA and protein expression, other regulatory mechanisms, such as translational efficiency and protein turnover rates (Nie et al., 2006) are likely to account for the observed dissociation between 5-HT_{2C}R mRNA and protein expression in the VTA.

The goat polyclonal anti-5-HT_{2C}R antibody (sc-15081; Santa Cruz Technology) utilized here has recently been shown to produce robust, consistent and replicable 5-HT_{2C}R-IR staining (Bubar et al., 2005) in mouse and rat brain that was consistent with findings with a home-generated 5-HT_{2C}R antibody (Clemett et al., 2000). The 5-HT_{2C}R-IR was eliminated in VTA sections taken from transgenic mice lacking the 5-HT_{2C}R gene relative to wild type mice and not observed in native CHO cells (which do not express the 5-HT_{2C}R protein) or CHO cells that expressed the closely related 5-HT_{2A}R (Bubar et al., 2005). These results suggest that the antibody binds to the 5-HT_{2C}R and does not cross-react with the 5-HT_{2A}R. In addition, a complete absence of immunostaining in control assessments of either the 5-HT_{2C}R primary antibody alone or the appropriate secondary antibody alone was observed in the current (data not shown) and previously published study (Bubar et al., 2005), suggesting that the IR detected is specific to the combination of 5-HT_{2C}R-specific primary and secondary antibodies.

Estimates of the total number of cells detected within the analyzed regions of interest in the VTA indicate that ~57% of labeled cells were TH-immunopositive while ~43% were GAD-immunopositive. These proportions suggest a greater number of DA than GABA neurons within the VTA. Electrophysiological studies have reported distributions ranging from 46% DA and 53% GABA (Yim and Mogenson, 1980) to 77% DA and 16% GABA (Johnson and North, 1992), while a previous immunohistochemical study suggested ~64% of VTA neurons were dopaminergic (Swanson, 1982). The range across studies may reflect variation in the expression of the two neuronal subtypes across the VTA subnuclei and/or rostro-caudal level. Indeed, the proportion of TH vs. GAD cells did vary across subnuclei, with TH-IR cells representing >62% of the total cells detected in the all levels of the PBP and in the CLi. Conversely, approximately equal numbers of TH- and GAD-IR cells were detected in the rostral and mid RLi and caudal PN. Thus, although DA neurons are generally more prominently represented in the VTA than are GABA neurons, the proportions of DA and GABA neurons vary according to subnuclear and rostro-caudal location.

The present report is the first to confirm that the 5-HT_{2C}R protein is localized to a subpopulation of GABA neurons within the VTA which corroborates the observation that the 5-HT_{2C}R mRNA co-localized with GAD mRNA in the VTA (Eberle-Wang et al., 1997). In addition, we revealed that the 5-HT_{2C}R is co-localized to a subpopulation of DA neurons in the VTA. A previous study failed to identify co-localization of 5-HT_{2C}R mRNA with TH mRNA in the VTA (Eberle-Wang et al., 1997). Although the 5-HT_{2C}R-IR was observed to co-localize within ~17–48% of all TH-IR cells detected across the VTA subnuclei in the present study, given that the level of 5-HT_{2C}R mRNA expression is lower (Eberle-Wang et al., 1997) than the level of 5-HT_{2C}R protein expression detected in the present study, it is plausible that the incidence of colocalization of 5-HT_{2C}R mRNA with TH mRNA may have been below the limits of detection of the *in situ* hybridization assay.

The 5-HT_{2C}R appears to be prominently distributed in the membrane and cytoplasm of both TH-IR and GAD-IR perikarya, with potential localization in neuronal processes. This type of cellular distribution is similar to that described for the 5-HT_{2C}R in the substantia nigra (Clemett et al., 2000) as well as for the closely related 5-HT_{2A}R in the VTA (Cornea-Hebert et al., 1999;Doherty and Pickel, 2000;Nocjar et al., 2002). The percentage of total 5-HT_{2C}R+GAD-IR cells varied only slightly among the different subnuclei, with the greatest abundance of co-localization detected in the middle level of the PBP. Conversely, the proportion of TH-IR cells containing 5-HT_{2C}R-IR significantly differed both across subnuclei and rostro-caudal levels. In general, the greatest incidence of co-localization for 5-HT_{2C}R+TH-IR was detected in the middle levels of PBP, PN and IF. Incidentally, these subnuclei are also reported to contain the greatest populations of neurons projecting to the NAc and PFC (Swanson, 1982). Furthermore, both DA (Swanson, 1982) and GABA neurons (Van Bockstaele and Pickel, 1995;Steffensen et al., 1998) in these subnuclei (PBP, PN, IF) are reported to project to the NAc and PFC. Thus, the present findings indicate that the 5-HT_{2C}R has the potential to directly influence both DA and GABA function in the mesocorticoaccumbens circuit.

Functional implications

The localization of the 5-HT_{2C}R to both GABA and DA neurons in the VTA suggests that the 5-HT_{2C}R has the potential to exert effects upon the output of this midbrain nucleus via multiple sites of action, although the functional roles of these distinct subpopulations of the 5-HT_{2C}R are difficult to predict. Stimulation of the 5-HT_{2C}R activates multiple signaling cascades. For example, 5-HT_{2C}R stimulation induces phospholipase C–mediated inositol phosphate accumulation and enhancement of intracellular Ca^{2+}, thereby depolarizing cell membranes to increase firing rates of neurons (Stanford et al., 2005). As such, stimulation of the 5-HT_{2C}R on GABA neurons, should escalate the firing rate of VTA GABA neurons, and would subsequently be expected to *reduce* the firing rate of local DA neurons, as one function of GABA neurons originating in the VTA is to inhibit the firing of local VTA DA neurons (Johnson and North, 1992). Indeed, microiontophoretic application of the nonselective 5-HT_{2C}R agonist *m*-chlorophenylpiperazine (mCPP) into the VTA increased the firing rate of non-DA (presumably GABA) neurons in the VTA (Di Giovanni et al., 2001) and also decreased the firing rate VTA DA neurons (Prisco et al., 1994). Conversely, stimulation of the 5-HT_{2C}R localized to DA neurons in the VTA would be expected to *increase* the firing rate of the DA neurons, although studies to isolate this recently discovered subpopulation of DA neurons possessing the 5-HT_{2C}R have yet to be conducted. Thus, it seems that stimulation of these two populations of VTA 5-HT_{2C}R is likely to exert opposing influences on the output of DA neurons. As such, the balance of influence exerted by these opposing subpopulations of 5-HT_{2C}R may be an important mechanism for regulation of VTA DA neuron output.

The differences in the distribution of TH- versus GAD-IR cells as well as the variations in the proportion of 5-HT_{2C}R-IR+TH-IR cells versus 5-HT_{2C}R+GAD-IR cells across subnuclei and

the rostro-caudal level, as observed in the present studies, suggest that the combined influence of the two subpopulations of the 5-HT_{2C}R on the output of DA neurons may vary along the rostro-caudal gradient and/or among the subnuclei of the VTA. Indeed, several studies have noted variations in the functional roles for other neurotransmitter receptors [e.g., GABA(A) receptor, glutamate GluR1 receptor] in rostral (−4.90 to −5.40 mm Bregma) compared with mid/caudal (−5.50 to −6.20 mm Bregma) regions of the VTA (Ikemoto et al., 1997, 1998;Carlezon et al., 2000;Olson et al., 2005). In addition, the effects of local administration of 5-HT_{2C}R ligands into the VTA are variable, possibly due to the anatomical location targeted. For example, electrophysiological studies in which microiontophoretic application of the nonselective 5-HT_{2C}R agonist mCPP was shown to increase and decrease the neuronal activity of DA- and GABA-containing cells, respectively, were conducted in the mid/caudal levels of the VTA (−5.60 to −6.30 mm Bregma; Prisco et al., 1994;Di Giovanni et al., 2001). Conversely, intra-VTA microinfusion of the *selective* 5-HT_{2C}R agonist RO 60,0175 into the rostral VTA (−4.80 to −5.30 mm Bregma) did not alter basal levels of DA measured in the NAc (Navailles et al., unpublished observations) or the PFC (Pozzi et al., 2002), nor did microinfusion of the 5-HT_{2C}R antagonists SB 206553 (Bankson and Yamamoto, 2004) or SB 242084 (Navailles et al., unpublished observations) into the rostral VTA (~−4.80 to −5.30 mm Bregma) alter basal DA release in the NAc. Thus it is plausible that discrete populations of the 5-HT_{2C}R in the VTA may tightly regulate the influence of the 5-HT_{2C}R upon DA neurotransmission. Further studies are needed, however, to examine how the differences in the topographical organization of the 5-HT_{2C}R throughout the various rostro-caudal levels and subnuclei of the VTA differentially mediate the output of DA neurons.

CONCLUSION

In summary, the present study is the first to demonstrate localization of the 5-HT_{2C}R protein on subpopulations of GABA and DA neurons in the VTA. Although the distribution of the 5-HT_{2C}R on these two neuronal subtypes appears to vary slightly among the rostro-caudal levels of the various subnuclei, the incidence of co-localization of the 5-HT_{2C}R with DA neurons appears to predominate in several subnuclei, particularly in the middle-VTA. While the functional implications of these differences in co-localization of 5-HT_{2C}R are currently unknown, these data suggest that the 5-HT_{2C}R control of VTA DA neuronal output may vary across subnuclei and/or rostro-caudal level. Further examination into the impact of these different 5-HT_{2C}R subpopulations through systematic microinfusion studies is necessary to fully understand how the 5-HT_{2C}R in the VTA regulates activation of the DA mesocorticoaccumbens pathways.

Acknowledgements

We would like to thank Erik J. Shank, Sonja J. Stutz, and Dr. Shijing Liu for assisting with image analysis. In addition, we appreciate the assistance of Dr. Thomas Albrecht and Mr. Eugene Knutson at the UTMB Infectious Disease and Toxicology Optical Imaging Core in conducting the confocal microscopy imaging. This research was supported by the National Institute on Drug Abuse DA 00260, DA 07287, DA 13595, DA 15259 and DA 20087. This manuscript was presented by M.J.B. in partial fulfillment of the requirements for the Ph.D. degree to the Graduate School of Biomedical Sciences at the University of Texas Medical Branch.

References

Abramowski D, Rigo M, Duc D, Hoyer D, Staufenbiel M. Localization of the 5-hydroxytryptamine2C receptor protein in human and rat brain using specific antisera. Neuropharmacology 1995;34:1635–1645. [PubMed: 8788961]

Bankson MG, Yamamoto BK. Serotonin-GABA interactions modulate MDMA-induced mesolimbic dopamine release. J Neurochem 2004;91:852–859. [PubMed: 15525339]

Bubar MJ, Cunningham KA. Serotonin 5-HT2A and 5-HT2C receptors as potential targets for modulation of psychostimulant use and dependence. Curr Top Med Chem 2006;6:1971–1985. [PubMed: 17017968]

Bubar MJ, Seitz PK, Thomas ML, Cunningham KA. Validation of a selective serotonin 5-HT(2C) receptor antibody for utilization in fluorescence immunohistochemistry studies. Brain Res 2005;1063:105–113. [PubMed: 16274677]

Cai L, Friedman N, Xie XS. Stochastic protein expression in individual cells at the single molecule level. Nature 2006;440:358–362. [PubMed: 16541077]

Carlezon WA Jr, Haile CN, Coppersmith R, Hayashi Y, Malinow R, Neve RL, Nestler EJ. Distinct sites of opiate reward and aversion within the midbrain identified using a herpes simplex virus vector expressing GluR1. J Neurosci 2000;20:RC62. [PubMed: 10684909]

Carr DB, Sesack SR. GABA-containing neurons in the rat ventral tegmental area project to the prefrontal cortex. Synapse 2000;38:114–123. [PubMed: 11018785]

Clemett DA, Punhani T, Duxon MS, Blackburn TP, Fone KC. Immunohistochemical localisation of the 5-HT2C receptor protein in the rat CNS. Neuropharmacology 2000;39:123–132. [PubMed: 10665825]

Cornea-Hebert V, Riad M, Wu C, Singh SK, Descarries L. Cellular and subcellular distribution of the serotonin 5-HT2A receptor in the central nervous system of adult rat. J Comp Neurol 1999;409:187–209. [PubMed: 10379914]

Dahlstrom A, Fuxe K. Localization of monoamines in the lower brain stem. Experientia 1964;20:398–399. [PubMed: 5856530]

Di Giovanni G, Di Matteo V, Di Mascio M, Esposito E. Preferential modulation of mesolimbic vs nigrostriatal dopaminergic function by serotonin(2C/2B) receptor agonists: a combined in vivo electrophysiological and microdialysis study. Synapse 2000;35:53–61. [PubMed: 10579808]

Di Giovanni G, Di Matteo V, La Grutta V, Esposito E. m-Chlorophenylpiperazine excites non-dopaminergic neurons in the rat substantia nigra and ventral tegmental area by activating serotonin-2C receptors. Neuroscience 2001;103:111–116. [PubMed: 11311791]

Di Matteo V, De Blasi A, Di Giulio C, Esposito E. Role of 5-HT(2C) receptors in the control of central dopamine function. Trends Pharmacol Sci 2001;22:229–232. [PubMed: 11339973]

Di Matteo V, Di Giovanni G, Di Mascio M, Esposito E. SB 242084, a selective serotonin2C receptor antagonist, increases dopaminergic transmission in the mesolimbic system. Neuropharmacology 1999;38:1195–1205. [PubMed: 10462132]

Doherty MD, Pickel VM. Ultrastructural localization of the serotonin 2A receptor in dopaminergic neurons in the ventral tegmental area. Brain Res 2000;864:176–185. [PubMed: 10802024]

Domesick VB, Stinus L, Paskevich PA. The cytology of dopaminergic and nondopaminergic neurons in the substantia nigra and ventral tegmental area of the rat: a light- and electron-microscopic study. Neuroscience 1983;8:743–765. [PubMed: 6408498]

Eberle-Wang K, Mikeladze Z, Uryu K, Chesselet MF. Pattern of expression of the serotonin2C receptor messenger RNA in the basal ganglia of adult rats. J Comp Neurol 1997;384:233–247. [PubMed: 9215720]

Fite KV, Wu PS, Bellemer A. Photostimulation alters c-Fos expression in the dorsal raphe nucleus. Brain Res 2005;1031:245–252. [PubMed: 15649450]

Hoffman BJ, Mezey E. Distribution of serotonin 5-HT1C receptor mRNA in adult rat brain. FEBS Lett 1989;247:453–462. [PubMed: 2714444]

Ikemoto S, Murphy JM, McBride WJ. Self-infusion of GABA(A) antagonists directly into the ventral tegmental area and adjacent regions. Behav Neurosci 1997;111:369–380. [PubMed: 9106676]

Ikemoto S, Murphy JM, McBride WJ. Regional differences within the rat ventral tegmental area for muscimol self-infusions. Pharmacol Biochem Behav 1998;61:87–92. [PubMed: 9715810]

Johnson SW, North RA. Two types of neurone in the rat ventral tegmental area and their synaptic inputs. J Physiol 1992;450:455–468. [PubMed: 1331427]

Kapur S, Remington G. Serotonin-dopamine interaction and its relevance to schizophrenia. Am J Psychiatry 1996;153:466–476. [PubMed: 8599393]

Keppel, G. Design and analysis: A researcher's handbook. Englewood Cliffs, NJ: Prentice-Hall, Inc; 1973.

Li QH, Nakadate K, Tanaka-Nakadate S, Nakatsuka D, Cui Y, Watanabe Y. Unique expression patterns of 5-HT2A and 5-HT2C receptors in the rat brain during postnatal development: Western blot and immunohistochemical analyses. J Comp Neurol 2004;469:128–140. [PubMed: 14689478]

Mengod G, Pompeiano M, Martinez-Mir MI, Palacios JM. Localization of the mRNA for the 5-HT2 receptor by in situ hybridization histochemistry. Correlation with the distribution of receptor sites. Brain Res 1990;524:139–143. [PubMed: 2400925]

Nie L, Wu G, Zhang W. Correlation of mRNA expression and protein abundance affected by multiple sequence features related to translational efficiency in Desulfovibrio vulgaris: A quantitative analysis. Genetics 2006;174:2229–2243. [PubMed: 17028312]

Nocjar C, Roth BL, Pehek EA. Localization of 5-HT(2A) receptors on dopamine cells in subnuclei of the midbrain A10 cell group. Neuroscience 2002;111:163–176. [PubMed: 11955720]

Olson VG, Zabetian CP, Bolanos CA, Edwards S, Barrot M, Eisch AJ, Hughes T, Self DW, Neve RL, Nestler EJ. Regulation of drug reward by cAMP response element-binding protein: evidence for two functionally distinct subregions of the ventral tegmental area. J Neurosci 2005;25:5553–5562. [PubMed: 15944383]

Paxinos, G.; Watson, C. The rat brain in stereotaxic coordinates. Sydney: Academic Press; 1998.

Phillipson OT. The cytoarchitecture of the interfascicular nucleus and ventral tegmental area of Tsai in the rat. J Comp Neurol 1979;187:85–98. [PubMed: 489779]

Pompeiano M, Palacios JM, Mengod G. Distribution of the serotonin 5-HT2 receptor family mRNAs: comparison between 5-HT2A and 5-HT2C receptors. Brain Res Mol Brain Res 1994;23:163–178. [PubMed: 8028479]

Pozzi L, Acconcia S, Ceglia I, Invernizzi RW, Samanin R. Stimulation of 5-hydroxytryptamine (5-HT (2C)) receptors in the ventrotegmental area inhibits stress-induced but not basal dopamine release in the rat prefrontal cortex. J Neurochem 2002;82:93–100. [PubMed: 12091469]

Prisco S, Pagannone S, Esposito E. Serotonin-dopamine interaction in the rat ventral tegmental area: an electrophysiological study in vivo. J Pharmacol Exp Ther 1994;271:83–90. [PubMed: 7965760]

Stanford IM, Kantaria MA, Chahal HS, Loucif KC, Wilson CL. 5-Hydroxytryptamine induced excitation and inhibition in the sub-thalamic nucleus: action at 5-HT(2C), 5-HT(4) and 5-HT(1A) receptors. Neuropharmacology 2005;49:1228–1234. [PubMed: 16229866]

Steffensen SC, Svingos AL, Pickel VM, Henriksen SJ. Electro-physiological characterization of GABAergic neurons in the ventral tegmental area. J Neurosci 1998;18:8003–8015. [PubMed: 9742167]

Swanson LW. The projections of the ventral tegmental area and adjacent regions: a combined fluorescent retrograde tracer and immunofluorescence study in the rat. Brain Res Bull 1982;9:321–353. [PubMed: 6816390]

Van Bockstaele EJ, Pickel VM. GABA-containing neurons in the ventral tegmental area project to the nucleus accumbens in rat brain. Brain Res 1995;682:215–221. [PubMed: 7552315]

Winterer G, Weinberger DR. Genes, dopamine and cortical signal-to-noise ratio in schizophrenia. Trends Neurosci 2004;27:683–690. [PubMed: 15474169]

Wise RA. Forebrain substrates of reward and motivation. J Comp Neurol 2005;493:115–121. [PubMed: 16254990]

Wright DE, Seroogy KB, Lundgren KH, Davis BM, Jennes L. Comparative localization of serotonin1A, 1C, and 2 receptor subtype mRNAs in rat brain. J Comp Neurol 1995;351:357–373. [PubMed: 7706547]

Yim CY, Mogenson GJ. Electrophysiological studies of neurons in the ventral tegmental area of Tsai. Brain Res 1980;181:301–313. [PubMed: 7350968]

Zhang Q, Andersen ME, Conolly RB. Binary gene induction and protein expression in individual cells. Theor Biol Med Model 2006;3:18. [PubMed: 16597340]

Abbrevations

CLi

caudal linear raphe nucleus

DA
dopamine

DAPI
4′,6-diamidoino-2-phenylindole

GAD
glutamic acid decarboxylase

IF
interfascicular nucleus

IP
interpeduncular nucleus

IR
immunoreactivity/immunoreactive

mCPP
m-chlorophenylpiperazine

NAc
nucleus accumbens

PBP
parabrachial pigmented nucleus

PBS
phosphate-buffered saline

PFC
prefrontal cortex

PN
paranigral nucleus

RLi
rostral linear raphe nucleus

RT
room temperature

TH
tyrosine hydroxylase

VTA
ventral tegmental area

5-HT
serotonin

5-HT$_{2C}$R
serotonin 2C receptor

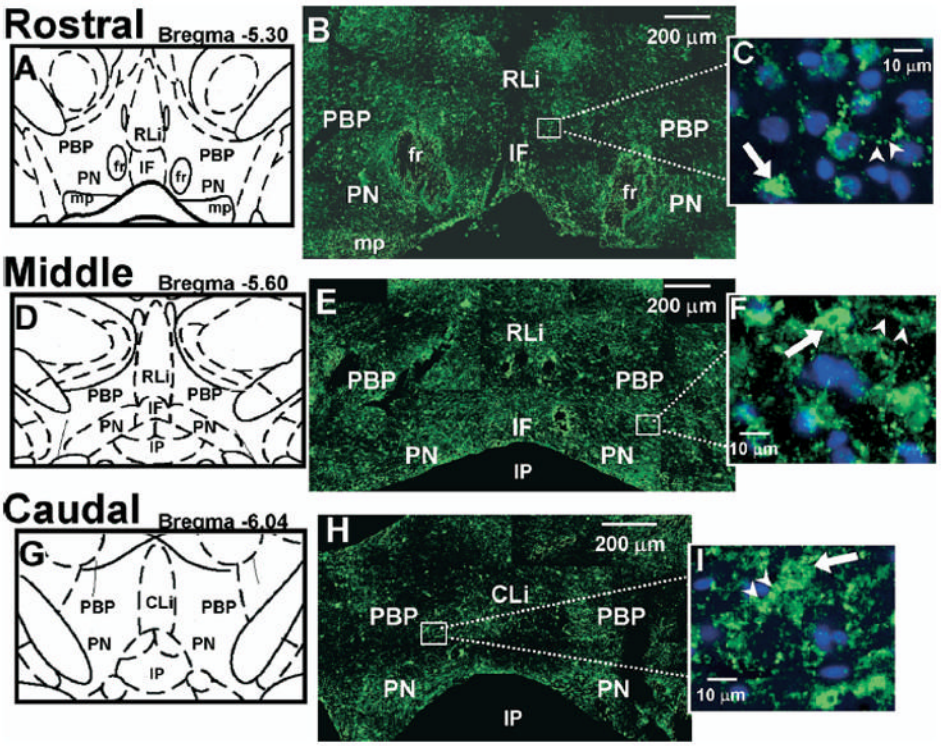

Fig 1.

5-HT_{2C}R IR in the VTA. (A, D, G) Schematic diagrams of the VTA subnuclei at rostral (Bregma −5.30 mm; A), middle (Bregma −5.60 mm; D), and caudal (Bregma −6.04 mm; G) levels of the VTA. (B, E, H) Representative composite photomicrographs displaying 5-HT_{2C}R IR (green) in rostral (B), middle (E) and caudal (H) levels of the VTA. (C, F, I) High magnification photographs of the boxed area in panels B, E, and H, respectively. DAPI-labeled nuclei are shown in blue. □, Examples of 5-HT_{2C}R-IR cell bodies (green); □, potential 5-HT_{2C}R-IR neuronal processes (green). Scale bars=200 μm (B, E, H); 10 μm (C, F, I). The five VTA subnuclei include: PBP, PN, IF, RLi, CLi. The location of the fasciculus retroflexus (fr), interpeduncular nucleus (IP), and mammillary peduncle (mp) is labeled for orientation purposes.

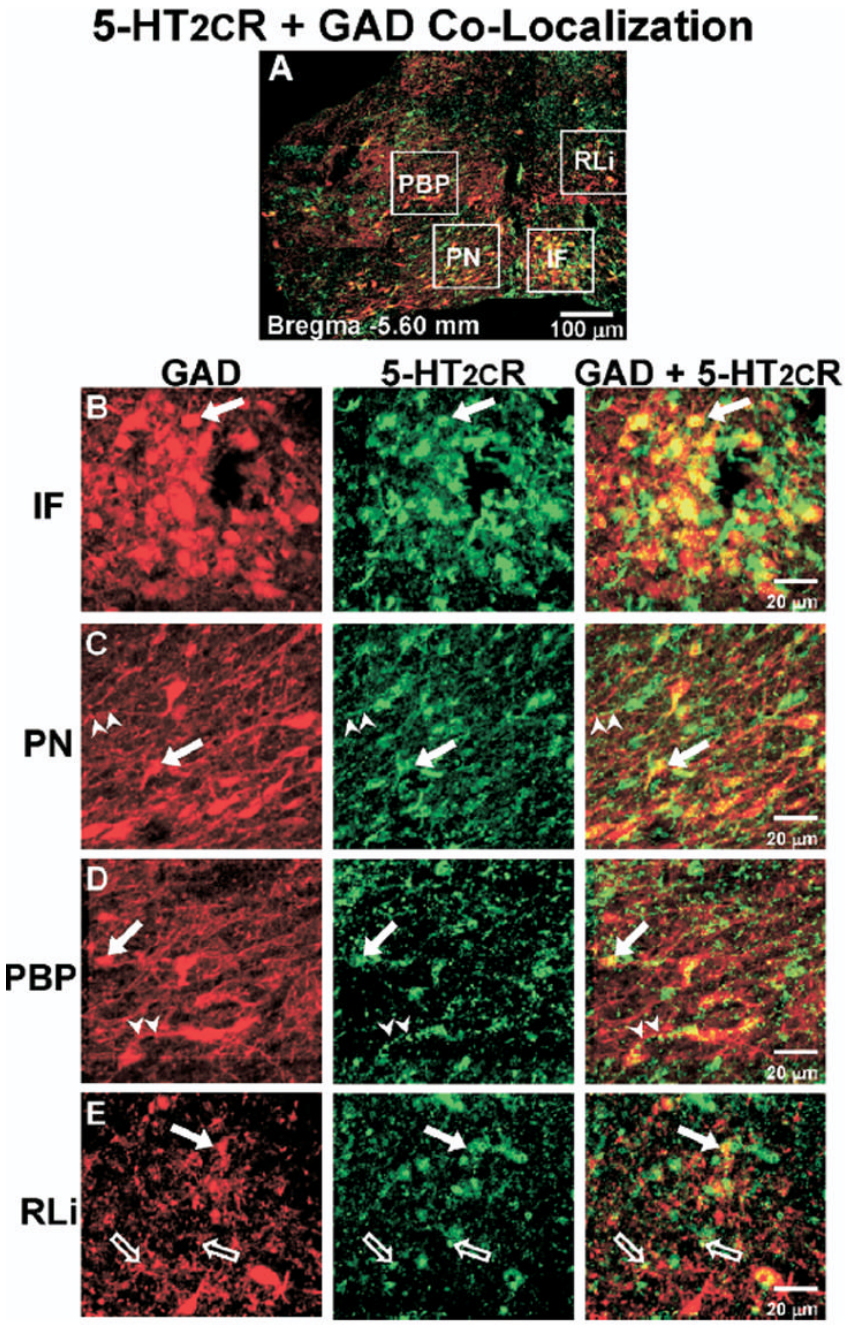

Fig 2.

Co-localization of 5-HT_{2C}R+GAD IR in the middle VTA. (A) Representative composite photomicrograph of the middle level of the VTA (Bregma −5.60 mm) displaying the overlay of GAD-IR (red) and 5-HT_{2C}R-IR (green); cells containing IR for both GAD and 5-HT_{2C}R appear yellow. (B–E) High magnification images of boxed areas in panel A, representing the various VTA subnuclei (see Fig. 1 for abbreviations). Left column, GAD-IR (red); middle column, 5-HT_{2C}R-IR (green); right column, overlay of images to demonstrate GAD and 5-HT_{2C}R co-localization (yellow). □, Indicate cell bodies containing both GAD and 5-HT_{2C}R-IR; □, co-labeled neuronal processes; □, potential terminal boutons. Scale bars=100 μm (A); 20 μm (B–E).

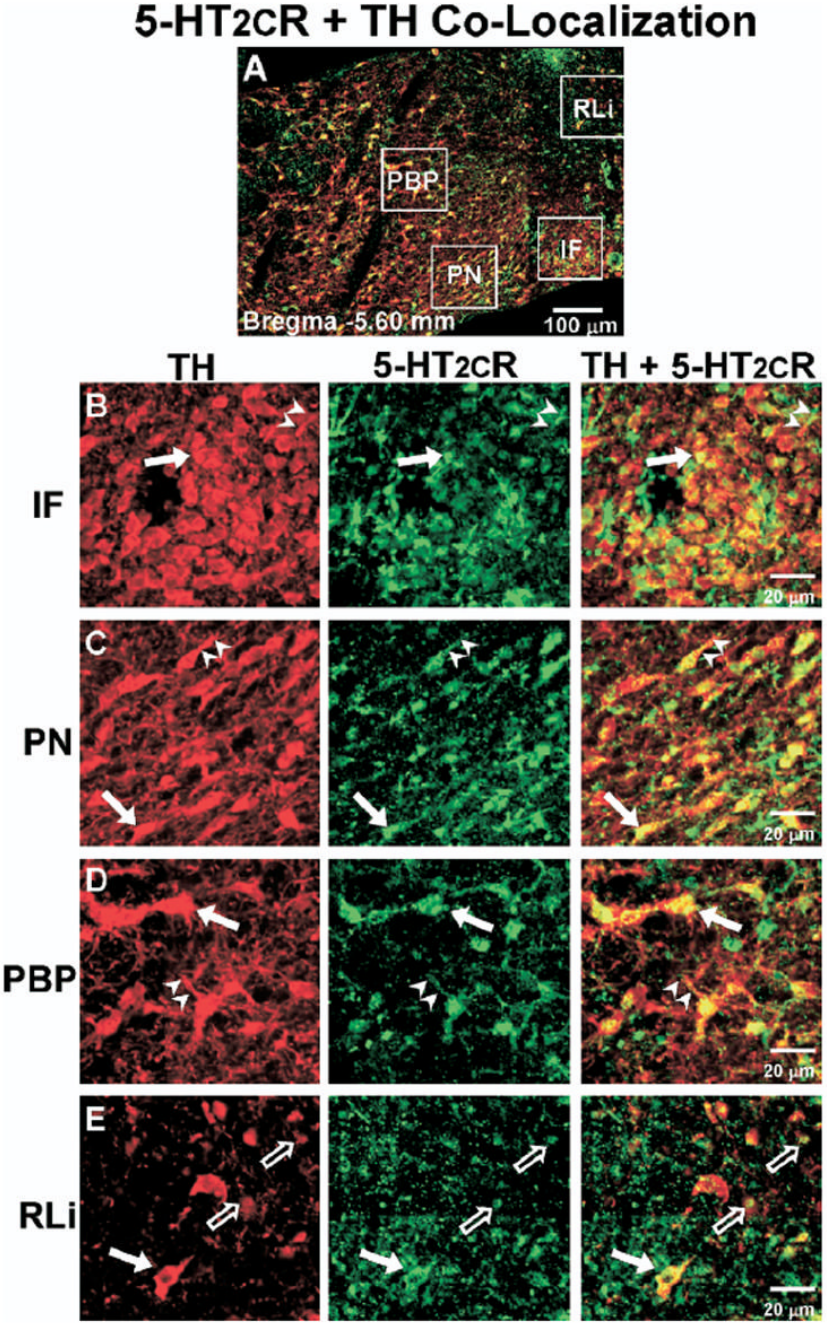

Fig 3.

Co-localization of 5-HT_{2C}R+TH IR in the middle VTA. (A) Representative composite photomicrograph of the middle level of the VTA (Bregma −5.60 mm) displaying the overlay of TH-IR (red) and 5-HT_{2C}R-IR (green); cells containing IR for both TH and 5-HT_{2C}R appear yellow. (B–E) High magnification images of boxed areas in panel A, representing the various VTA subnuclei (see Fig. 1 for abbreviations). Left column, TH-IR (red); middle column, 5-HT_{2C}R-IR (green); right column, overlay of images to demonstrate TH and 5-HT_{2C}R co-localization (yellow). □, Indicate cell bodies containing both TH and 5-HT_{2C}R-IR; □, co-labeled neuronal processes; □, potential terminal boutons. Scale bars=100 μm (A); 20 μm (B–E).

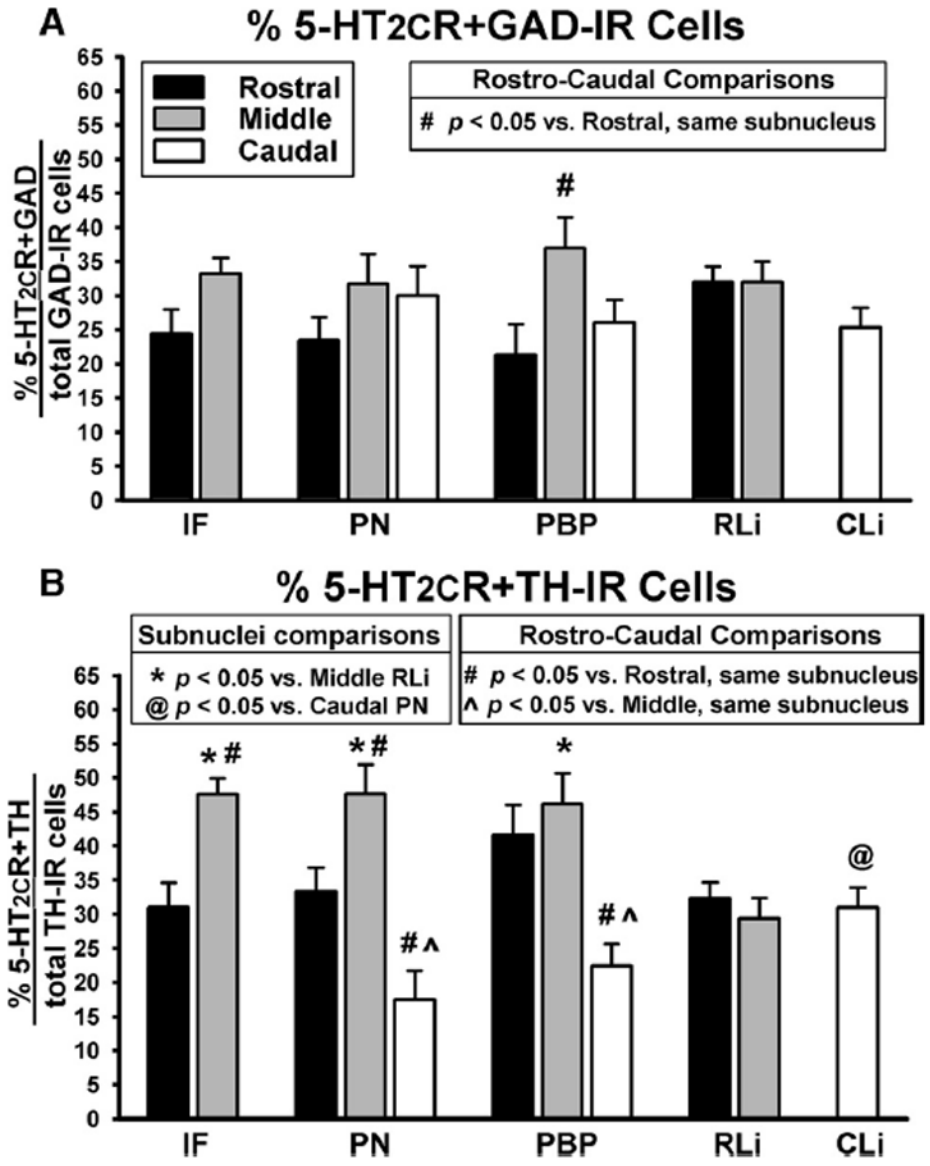

Fig 4.

Percentage of 5-HT$_{2C}$R+GAD and 5-HT$_{2C}$R+TH co-localized cells in the various VTA subnuclei. Data represent the mean (±S.E.M.; *n*=7–12/group) percentage of (A) 5-HT$_{2C}$R +GAD co-localized cells and (B) 5-HT$_{2C}$R+TH co-localized cells in the rostral (black bars), middle (gray bars) and caudal (white bars) levels of the VTA subnuclei. Data were calculated by dividing the % of co-labeled cells by the total number of GAD- or TH-labeled cells, respectively, in each subnucleus for each VTA tissue section. Resultant values were averaged for the rostral, middle and caudal levels of each subnucleus. For analyses comparing the expression of co-localization among the different rostro-caudal levels of each subnucleus: $^{\#}$ *P*<0.05 compared with the rostral level of the same subnucleus; *P*<0.05 vs. middle level of the same subnucleus. For analyses comparing the expression of co-localization between the various subnuclei for each rostro-caudal level: * *P*<0.05 vs. middle RLi; $^{@}$ *P*<0.05 vs. caudal PN.

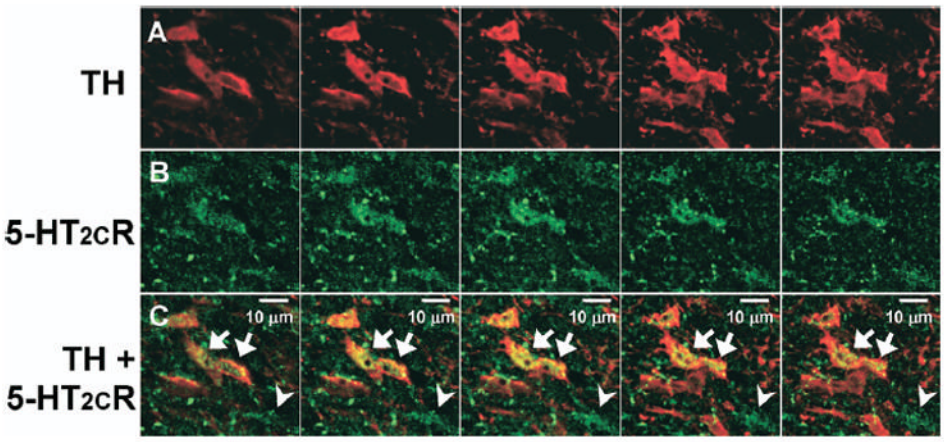

Fig 5.

Co-localization of TH and 5-HT_{2C}R IR. Series of five sequential photomicrographs (from left to right) captured using a confocal microscope displaying TH (A; red) and 5-HT_{2C}R (B; green) IR in the VTA. (C) Overlay of images in A and B shows co-localization of TH+5-HT_{2C}R IR (yellow) as indicated by arrows. Arrowheads point to a 5-HT_{2C}R-IR cell that is devoid of TH-IR. Scale bar=10 μm.

Table 1

Total number of TH-GAD- and 5-HT_{2C}R-immunoreactive cells detected in the various VTA subnuclei[a]

Subnucleus	Bregma Location[b]	TH-immunoreactive cells[c]	GAD-immunoreactive cells[d]	5-HT_{2C}R-immunoreactive cells[e]
IF				
Rostral	−5.00 to −5.40	79.18±3.52	64.36±7.36	67.23±4.26
Mid	−5.50 to −5.80	107.82±11.12	84.56±8.20	96.05±6.55
PN				
Rostral	−5.00 to −5.40	107.45±8.87	100.50±11.65	110.71±9.12
Mid	−5.50 to −5.80	157.00±16.87	112.91±10.18	133.91±9.01
Caudal	−5.90 to −6.30	80.25±12.85	83.50±8.06	87.31±8.44
PBP				
Rostral	−5.00 to −5.40	132.73±9.09	88.70±11.45	107.05±6.51
Mid	−5.50 to −5.80	141.08±12.88	99.22±6.49	124.62±7.55
Caudal	−5.90 to −6.30	109.29±13.71	91.88±8.54	73.73±7.07
Rli				
Rostral	−5.00 to −5.40	60.55±5.56	71.82±6.49	78.73±4.77
Mid	−5.50 to −5.80	69.33±4.91	63.36±5.26	80.95±6.38
Cli				
Caudal	−5.90 to −6.30	116.88±10.30	73.14±6.73	76.33±7.70

[a] Two separate regions of similar size (64.52 cm^2 each) were used in all levels for the PN and PBP; a single region was used for all levels of the IF(58.06 cm^2), RLi (58.06 cm^2), and Cli (64.52 cm^2).

[b] Bregma locations according to the brain atlas of Paxinos and Watson (1998).

[c] TH: average of 10–12 rostral and midsections, 8–9 caudal sections collected from 3 rats.

[d] GAD: average of 9–11 rostral and mid sections, 7–8 caudal sections collected from 3 rats.

[e] 5-HT_{2C}R: average of 21–122 rostral and mid sections, 15–116 caudal sections collected from 3 rats.